

Efficient H₂ Production via Novel Molecular Chromophores and Nanostructures

Arthur J. Nozik; Arthur J. Frank, co-PI
National Renewable Energy Laboratory
1617 Cole Bld
Golden, CO 80401
Ph: 303 384 6603; Fax: 303 384 6655
anozik@nrel.gov

DOE Program Officer: Richard Greene
richard.greene@science.doe.gov; 301 903 6190

Subcontractors:

Professor Josef Michl, University of Colorado, Boulder (1 graduate student); michl@eefus.colorado.edu

Objectives:

The objective of this research is to establish the fundamental science that will ultimately allow the construction of a high efficiency tandem photoelectrolysis solar cell (photoactive cathode and anode). The highest theoretical photolytic water splitting efficiency requires two photosystems (labeled PSI and PSII) that are coupled such that the two individual photopotentials are additive (like in biological photosynthesis) to generate sufficient voltage to split water into H₂ and O₂. Initial work is focused on generating two electron-hole pairs per photon via molecular singlet fission (SF) in novel dimeric chromophores that can sensitize the nanocrystalline TiO₂ cathode for H₂O reduction to H₂, and novel nanocrystalline anodic films that can support quantum dot sensitizers that exhibit efficient multiple exciton generation and can also oxidize H₂O to O₂. Doubling of the exciton production per photon will greatly increase the photocurrent and result in a relative maximum efficiency gain of about 33%.

Technical Barriers:

The technical barriers are to: (1) theoretically design, synthesize, and characterize novel molecular chromophores that exhibit efficient singlet fission and which can efficiently inject electrons from the biexcitonic state into nanocrystalline TiO₂; (2) discover and synthesize novel nanocrystalline supports for the cell anode that can accept injected photogenerated holes from QDs or other molecular chromophores and subsequently inject these holes into water to photooxidize H₂O to O₂, and (3) effectively couple the two photosystems through a charge conducting medium such that holes from the cathode sensitizer recombine with electrons from the cathode to maintain charge neutrality and current continuity in the cell; and (4) discover and develop all of these cell components with the appropriate values of redox potentials, electron affinities, bandgaps, particle size, morphology, and charge transfer kinetics to allow the cell to function.

Abstract

This work involves a basic research program that will ultimately enable new solar technology for a highly efficient and low cost water splitting system. The system consists of a unique tandem cell where the sunlight is first incident upon a photocathode, and light transmitted through the photocathode is absorbed in the photoanode. The photocathode generates two electrons per absorbed photon through singlet fission in unique molecular chromophores bound to a nanocrystalline TiO₂ support. The photoanode consists of hole-injecting molecular

chromophores or semiconductor quantum dots supported on a hole-conducting nanocrystalline film. If the photoanode also generates two electrons per absorbed photon through singlet fission or multiple exciton generation (MEG) in semiconductor quantum dots, the maximum cell efficiency for water splitting at zero overvoltage is 46%. A tandem cell with two photoelectrodes both producing just one electron per absorbed photon has a maximum efficiency of 40% at zero overvoltage; a cell with just one photoelectrode has a maximum efficiency of about 32% independent of whether one or two electrons are produced per absorbed photon.

Progress Report

Investigations of Singlet Fission in Designed Chromophores

Theoretical investigations: Chromophores based on ground state biradicals (Collaboration with J. Michl and M. Ratner)

Our approach considered that the lowest triplet state energy should be energetically below half the HOMO-LUMO energy gap. This removes the necessity for the SF process to compete with vibrational relaxation and instead allows SF to proceed through the vibrationally-relaxed S_1 state. The reverse of SF, T-T annihilation to produce S_1 , is also suppressed in this scheme because this process would be endoergic. Although most closed shell molecules do not have an S-T splitting (2 times the exchange energy) that approaches half the energy of the S_1 - S_0 gap, alternant hydrocarbons (polyacenes in particular) may fulfill such criteria, primarily because they have large ground and excited state orbital amplitudes on the same atoms. Another class of molecules that fulfill our criteria are homosymmetric biradicaloids. Although perfect biradicals are typically unstable (ground state of two electrons in two degenerate orbitals), molecules that are based upon biradicals but altered in order to produce stability (biradicaloids) may retain the large S_1 - T_1 gap while possessing electronic and optical properties suitable for spectroscopic studies and eventual use in practical devices.

A suitable method for canvassing the T_1 and T_2 energies of a large number of candidate molecules with reasonable accuracy is the semiempirical PPP method. This method was applied to alternant hydrocarbons (polyacenes, perylene diimides) and biradicaloids based upon the biradicals *p*-xylylene and *o*-xylylene. The S_1 , T_1 , and T_2 energies of nearly 70 molecules were calculated in this fashion. For the most relevant molecules, density functional theory (DFT) was used to provide more accurate results for the energies. Although several promising candidates were identified, the molecule 1,3-diphenylisobenzofuran (DPIBF) was chosen as an appropriate starting point for further studies of SF in molecular dimers.

Photophysical characterization of covalently-bound dimers

The DPIBF monomer and three covalent dimers were prepared according to procedures soon to be published. The absorption and fluorescence spectra are shown in Figure 1. **1** does not form triplets when excited directly (ISC rate is very slow), but it can be sensitized with anthracene to form triplets through T-T energy transfer. The T_1 - T_n absorption spectrum (obtained both by steady-state and time-resolved methods) has a peak near 460 nm. Although **2-4** have absorption and fluorescence features similar to **1**, there is a clear red-shift of the absorption as stronger coupling between monomeric units is induced. The strongest coupling occurs in **4**, in which the monomeric units are directly connected and no hindering groups are present to prevent planarity of the two halves and potential extension of the conjugation over both DPIBF chromophores. This molecule has significantly different photophysical properties compared with **2** and **3**. Most noteworthy are the trends in fluorescence and triplet quantum yields with the degree of interchromophore coupling and solvent polarity.

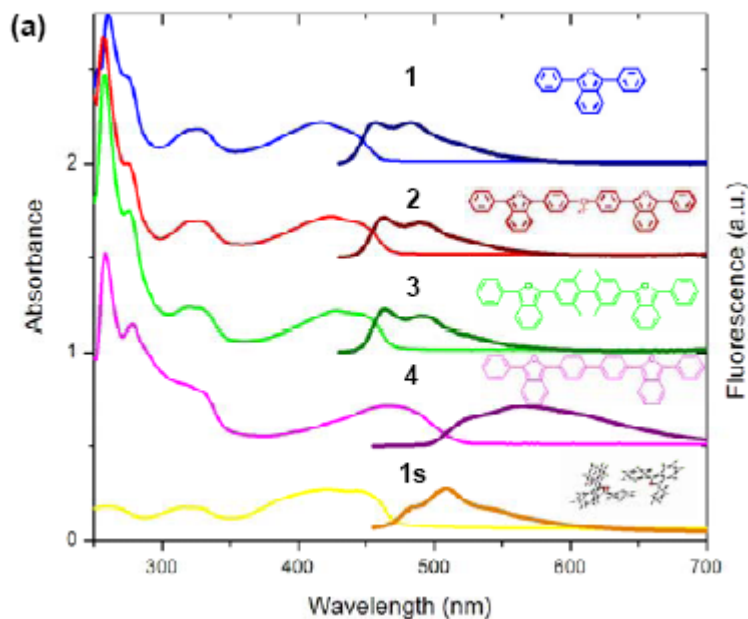


Figure 1 (a) Absorption and fluorescence for **1-4** in DMSO and the crystalline solid of **1** (**1s**). Molecular and crystal structures are inset. Spectra are offset for clarity. (b) Table of photophysical data. P (NP) is (non)polar solvent. τ_{ave} is the average fluorescence decay time (**2**, **3** in P solvent, and **4** and **1s** are multiexponential). τ_{form} (τ_{dec}) is the formation (decay) time of the triplet.

Triplet quantum yields (TQY) were measured in both the steady-state and with flash photolysis by collecting the T_1 - T_n absorption spectrum with and without a sensitizer (typically anthracene). Comparison of the amplitude of the absorption (with appropriate corrections) yields a quantitative value for the TQY and also, from the time-resolved data it is clear that the triplet lifetime is at least 200 ns for **1-3**, nearly 4 orders of magnitude longer than that of the singlet. The TQY is largest in **3** (about 6% at 300K and 9% at 250 K), which is the dimer with a direct connection between neighboring chromophores but hindering groups to prevent planarity. It is also clear that the TQY yield increases dramatically in polar solvents and is nearly zero in nonpolar solvents. For comparison, the TQY in **4** is not strongly dependent upon solvent, while the TQY for the monomer remains essentially zero.

The mechanism of triplet formation clearly involves cooperation between both chromophores in the dimer in the presence of a polar environment. Femtosecond transient absorption (TA) was performed on all molecules in a variety of solvents to help elucidate this mechanism. Time-resolved spectra were collected, and the data were fit globally to various proposed kinetic schemes. The best fits resulted from a kinetic scheme involving transformation from the locally-excited (LE) singlet to a polar intermediate S^* (and the reverse process), followed by either internal conversion of S^* to the ground state or conversion to a triplet (either ISC or SF). The species associated decay spectra clearly indicate the formation of triplets (with a rate constant near 1.5 ns) and the radical-ion pair with a rate constant near 250 ps. No emission occurred from the polar intermediate state, nor was a possible charge-separated triplet identified during these studies, making quantitative analysis of the $S^* \rightarrow T$ yield and mechanism difficult. However, an estimated yield obtained from measuring extinction coefficients for each species did not suggest a value considerably higher than unity for this process (indicating ISC may be the dominant triplet formation mechanism). SF may indeed still be occurring in these dimers, but higher accuracy would be required to measure this quantitatively, and in any case the overall yield would likely be only one or two percent at best.

Characterization of crystalline DPIBF properties

The crystal structure of the DPIBF monomer was obtained by X-ray diffraction and is shown in the inset of Figure 1. It is evident that despite the lack of covalent bonding, large co-facial coupling can be engendered through the close-packed molecular structure. Thin solid films of DPIBF exhibit significant TQY, possibly above ten percent. A quantitatively accurate value of the TQY is difficult to obtain due to uncertainty and irreproducibility in solid film properties (including those of standards used for reference). However, the presence of a large number of triplets in the nonpolar environment suggests that SF may be active. Current studies are aimed at quantifying the TQY and elucidating the triplet formation mechanism. Triplet formation is fast and multiexponential (formation

times of < 1 ps and 5-50 ps), considerably faster than triplets formed in solutions of covalently-bound dimers. Some T-T decay ($\sim 50\%$ of total) in the first ns could be due to annihilation of nascent triplets, while much longer lived triplets (> 100 ns) are able to diffuse from each other after SF. TA studies are underway to confirm the presence of SF in the crystal and to elucidate the detailed mechanism. If SF in crystals can be efficient, collecting multiple charge carriers per absorbed photon in nanocrystals and/or aggregates adsorbed to TiO_2 is a potentially viable route to achieve high photoconversion efficiencies.

New Nanocrystalline Hole Conductors for the Photoanode

Ordered photonic nanocrystalline supports (CdSe and Cu_xO)

One of our objectives was to develop porous hole conducting nanocrystalline semiconductor supports to capture photogenerated holes from the ground electronic state of optically excited chromophores (sensitizers) (e.g., QDs and molecular dyes) and transport them to the hole collecting substrate, which contacts a dark catalytic anode for water oxidation. Toward that end, we have been developing synthetic protocols for preparing ordered photonic nanocrystalline films as hole conductors. Ordered polystyrene (PS) bead films were prepared as templates for directing the growth of ordered porous semiconducting materials. We developed the methodology to deposit 3–4 μm thick films of 300, 400, and 500 nm PS beads arranged in a hexagonal close-packed array with periodic porosity. The film deposition conditions were found to be crucial for creating ordered self-assembled structures of PS beads on the nanometer scale. The orientation of the conducting substrate used during film drying affected significantly the architectural order. The angle of orientation was varied from 0 to 90° . Orienting the substrates vertically during film growth produced the most structurally ordered films. Finally, the most ordered films were obtained with conducting substrates that were treated to obtain good hydrophilicity and that had a high roughness factor.

The PS bead films were used as templates for depositing inverse opal (photonic crystal) semiconductor films via electrodeposition. Photonic crystals contain regularly repeating internal regions of high and low dielectric constants. This structural periodicity gives photonic crystals distinct optical properties (e.g., nonlinear dispersion – localization of light in either the high or low dielectric part of the material) that can be tuned to different wavelengths simply by changing the periodicity. X-ray diffraction data indicates that the as-deposited CdSe is the crystalline cubic phase and has an average size of 7.1 nm. Optical absorption measurements showed that the as-deposited CdSe exhibits a bandgap of about 1.75 eV, close to the bandgap of bulk CdSe. The latter observation is consistent with theoretical calculations of the Bohr radius (5.4 nm) for CdSe.

Incident-photon-to-current-conversion-efficiency (IPCE) measurements suggest that photoexcited PbSe QDs adsorbed onto the surface of these inverse opals inject holes into the CdSe support. Importantly, these data are also consistent with the CdSe matrix serving as a photonic crystal, as manifested by an enhancement of the photoresponse of the PbSe QDs at wavelengths of light corresponding to about double the pore diameter. Initial IPCE measurements and other data indicate that (a) as-deposited CdSe films are p-type, which facilitates hole transport to the conducting substrate, and that (b) the valence band edge of CdSe lies between the ground electronic state of the optically excited PbSe QDs ($E_g = 0.98$ eV for ca. 3.5 nm size particles) and the water-oxidation potential.

Polystyrene bead templates were also used to prepare inverse opal photonic crystals of copper oxide (Cu_xO). Both cuprous oxide (Cu_2O ; $E_g = 2.1$ eV) and cupric oxide (CuO ; $E_g = 1.4$ eV) are promising materials for photoanode materials because they appear to have the proper energy levels, are intrinsically p-type, and are environmentally benign. We have developed the electrodeposition conditions necessary for preparing inverse opal films composed of the cubic phase of Cu_2O , which is readily converted to monoclinic CuO upon heating in air. Our results suggest that the photonic crystal properties of the Cu_2O films may be tuned to enhance the light-harvesting efficiency of quantum dots or molecular sensitizers adsorbed to the surface of the films.

Hole-conducting nanocrystalline films of zinc chalcogenides

The oxidation half of the tandem water splitting cell requires a dye-sensitized, hole-conducting nanocrystalline film to complement the dye-sensitized nanocrystalline TiO_2 film used for water reduction. Here, an adsorbed dye injects holes into a wide band gap nanocrystalline material, which must then transport the holes to an outer interface with water in order to evolve oxygen. In addition to a wide band gap, the hole-conducting material should (i) possess a valence band deeper in energy than the oxidation potential of water, (ii) show intrinsic or *p*-type conduction, (iii) be readily sensitized by a suitable hole-injecting dye and (iv) be stable in the electrolyte used to couple the oxidation and reduction halves of the Zinc chalcogenides, especially ZnSe and $\text{ZnTe}_x\text{Se}_{1-x}$, are particularly promising, and can easily be prepared as high-quality colloidal nanocrystals.

In addition to CdSe and Cu_xO , the zinc chalcogenides, especially ZnSe and $\text{ZnTe}_x\text{Se}_{1-x}$, are particularly promising, and can easily be prepared as high-quality colloidal nanocrystals. We have fabricated nanocrystalline films from colloidal ZnSe , ZnS and ZnTe nanocrystals that are suitable for studying dye-sensitized hole injection and hole transport. We prepare 2–3 μm -thick films of these nanocrystals by spin coating from very concentrated solutions, and then use thermal or amine-based chemical treatments to controllably remove the layer of electrically-insulating oleate ligands initially present on their surface. A suite of techniques, including FTIR, XPS, SEM, x-ray scattering, ellipsometry, absorption spectroscopy and field-effect transistor measurements are used to characterize the films as a function of these treatments, with the aim of making carbon-free, sintered nanocrystalline films capable of anchoring large amounts of dye and transporting holes across the film thickness.

Thermodynamic Efficiencies of Water Splitting Devices

Tandem PEC devices have the potential to increase the efficiency of solar driven water splitting, with a limiting value of $\sim 40\%$ calculated for normal $\text{QY}=1$ absorbers. Exciton multiplication (EM) in tandem two-photosystem cells can be expected to increase the available current while maintaining a sufficiently high potential to drive the water splitting reaction, thereby increasing the overall conversion efficiency.

We first considered the efficiency of a tandem water splitting cell having M1 absorbers in both the top and bottom cells versus the bottom cell band gap, E_2 . The top cell band gap, E_1 was chosen to maximize the efficiency. The maximum efficiency under the ideal condition of $V_0 = 0$ V is 40.0% and occurs with top and bottom cell gaps of 1.40 eV and 0.52 eV, respectively. As the overpotential increases to 0.4 and 0.8 V, the maximum efficiency decreases to 33.2% and 27.1%, respectively, while the optimum top and bottom cell gaps move to higher energies. We find similar trends in plots of maximum efficiency and $E_{1\text{max}}$ for tandem water splitting cells with MEG absorbers. The maximum efficiency for the tandem PEC device with a SF top cell and M1 bottom cell is 42.7% which decreases to 33.4% and 23.6% for $V_0 = 0.4$ V and 0.8 V, respectively. For a tandem water splitting cell with a SF top cell and M2 bottom cell, the maximum efficiency is 46.0% which decreases to 33.4% and 23.6% for $V_0 = 0.4$ V and 0.8 V, respectively. The cell configuration with both the anode and cathode producing two excitons/photon (either via SF or MEG in QDs) yields the highest theoretical water splitting efficiency (46%), and at $V_0 = 0$ V represents a 15% increase over cells with no exciton multiplication.

However, the introduction of overvoltage losses in water splitting cells shows that cells with exciton multiplication lose their advantage over normal water splitting cells for overpotentials above $V_0 \sim 0.4$ V. In At low overpotentials, single-gap and tandem devices with MEG absorbers have higher efficiencies than devices without MEG. For single-gap devices, the efficiency of the M1 and M2 devices become equal above $V_0 \sim 0.4$ V. As V_0 increases, larger band gaps for both the top and bottom cells in a tandem device are required to obtain sufficient photovoltage to overcome the losses and drive the water splitting reaction.

One very important aspect of our solar water splitting system is that under one sun illumination intensity (no solar concentration) the current densities are rather low (for example, 20 mA/cm^2 for a 25% efficient cell), and this translates to low overvoltages. At 20 mA/cm^2 , the overvoltage for water splitting at platinum electrodes is only about 0.11 V; it only increases to 0.15 V at 40 mA/cm^2 . This makes the problem of producing the required low overvoltages in our novel cells much easier.

Publications

1. I. Paci, J.C. Johnson, X. Chen, G. Rana, D. Popovic, D.E. David, A.J. Nozik, M. A. Ratner, J. Michl, Singlet Fission for Dye-Sensitized Solar Cells: Can a Suitable Sensitizer Be Found? Paci, I.; Johnson, J. C.; Chen, X.; Rana, G.; Popovic, D.; David, D. E.; Nozik, A. J.; Ratner, M. A.; Michl, J. *J. Am. Chem. Soc.*; **128**; 16546 (2006).
2. Hanna, M.C. and A.J. Nozik, "Solar Conversion Efficiency of Photovoltaic and Photoelectrolysis Cells with Carrier Multiplication Absorbers," *J. Appl. Phys.* **100**, 074510, 8 pages (2006).
3. Murphy, J.E., M.C. Beard, A.G. Norman, S.P. Ahrenkiel, J.C. Johnson, P. Yu, O.I. Mićić, R.J. Ellingson and A.J. Nozik, "PbSe Colloidal Nanocrystals: Synthesis, Characterization, and Multiple Exciton Generation," *J. Am. Chem. Soc.* **128**, 3241–3247 (2006).
4. Ellingson, R.J., M.C. Beard, J. Johnson, P. Yu, O.I. Mićić, A.J. Nozik, A.J. Shaehev and A.L. Efros, "Highly Efficient Multiple Exciton Generation in Colloidal PbSe and PbS Quantum Dots," *Nano Lett.* **5**, 865–871 (2005).
5. Schwerin, A., Johnson, J., A. Nozik and J. Michl, "Toward Designed Singlet Fission. 1. Electronic Excitation in 1,3-Diphenylisobenzofuran," to be submitted.
6. Johnson, J., X. Chen, A. Akdag, D. Popovic, G. Rana, M. Ratner, A. Nozik and J. Michl, "Toward Designed Singlet Fission. 2. Solution Photophysics of Three Covalent Dimers of 1,3-Diphenylisobenzofuran," to be submitted.
7. Johnson, J., A. Schwerin, A. Nozik and J. Michl, "Toward Designed Singlet Fission. 3. Solid-State Photophysics of 1,3-Diphenylisobenzofuran and Its Covalent Dimers," to be submitted.